



# Validation of Cirrus Cloud Properties Derived from CALIPSO

Matthew McGill, Dennis Hlavka, John Yorks, NASA GSFC  
Mark Vaughan, Sharon Rodier, Ralph Kuehn, NASA LaRC  
Stuart Young, CSIRO



The CALIPSO satellite provides the science community with data relevant to climate system studies, to permit studies of global cloud statistics and investigations of cloud-aerosol radiative effects.

Cirrus cloud optical properties (e.g., optical depth, extinction) derived from CALIPSO data were compared to similar data obtained using the airborne Cloud Physics Lidar (CPL) operating on the high-altitude ER-2 aircraft.

A series of 10 flights were conducted in the summer of 2006 using the CPL to provide collocated data to validate the CALIPSO measurements.

Results indicate that for cirrus clouds the lidar ratio (ratio of extinction to backscatter) and the retrieved extinction compare favorably between the two instruments, thereby validating the CALIPSO retrievals. In general, retrievals of optical depth agree to within ~7%, which is spectacular for lidar intercomparisons.

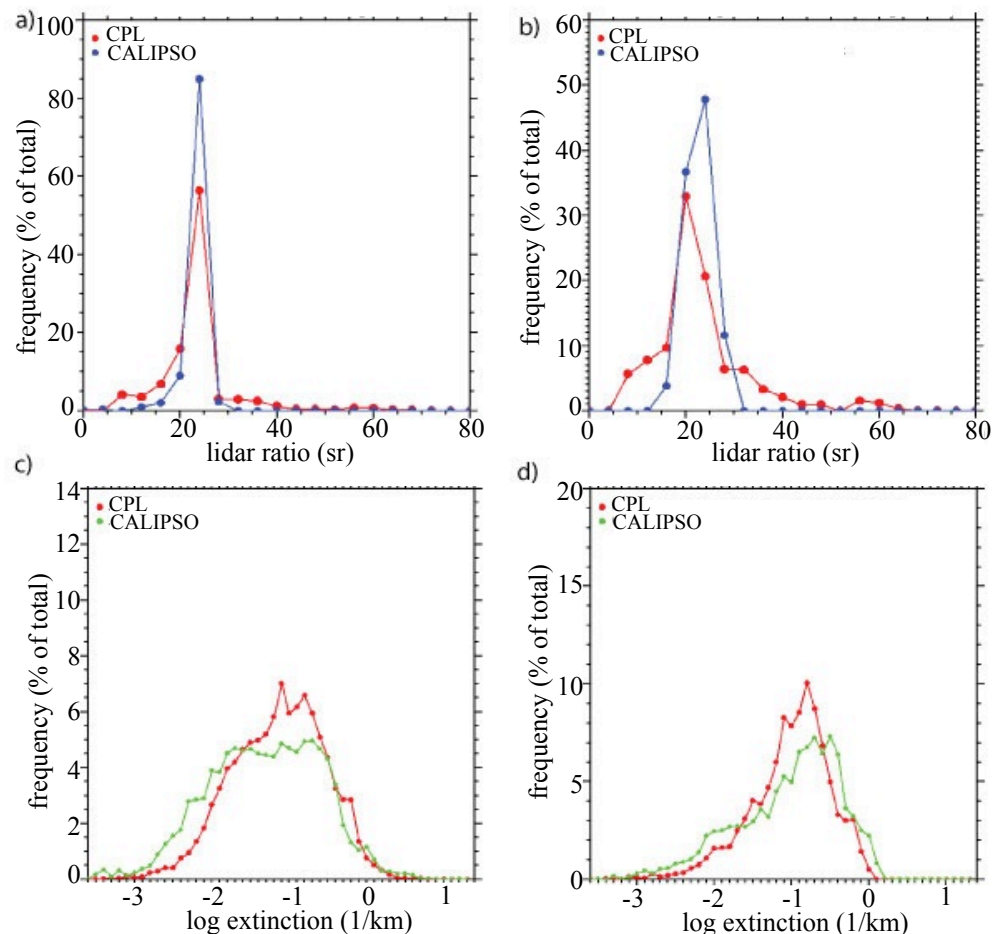


**Figure 1.** Frequency distributions of lidar ratio from CPL (red) and CALIPSO (blue), from periods of coincident measurement (restricted to cases of cirrus with randomly-oriented ice conditions only). (a) shows the composite distribution of all data and (b) shows the nighttime-only distribution. (c) and (d) show the corresponding extinction distributions for CPL (red) and CALIPSO (green) for the same composite and nighttime-only distributions, respectively. There is some difference evident from day to night, although exact reasons for the difference are not apparent.



Name: Matthew McGill, NASA/GSFC, Code 612

E-mail: Matthew.J.McGill@nasa.gov

Phone: 301-614-6281

## References:

Hlavka, D.L., J.E. Yorks, S. Young, M. Vaughan, R. Kuehn, M. McGill, and S. Rodier, "Airborne Validation of Cirrus Cloud Properties Derived from CALIPSO Lidar Measurements: Optical Properties," *Journal of Geophysical Research* (2012, *in review*).

Yorks, J. E., D. L. Hlavka, M. A. Vaughan, M. J. McGill, W. D. Hart, S. Rodier, and R. Kuehn, "Airborne validation of cirrus cloud properties derived from CALIPSO lidar measurements: Spatial properties," *Journal of Geophysical Research*, **116**, D19207, doi:10.1029/2011JD015942 (2011).

McGill, M. J., M. A. Vaughan, C. R. Trepte, W. D. Hart, D. L. Hlavka, D. M. Winker, and R. Kuehn, "Airborne validation of spatial properties measured by the CALIPSO lidar," *Journal of Geophysical Research*, **112**, D20201, doi:10.1029/2007JD008768 (2007).

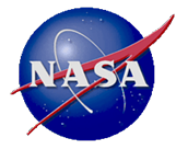
**Data Sources:** The 5 km horizontal resolution cloud layer products from Cloud-Aerosol Lidar Infrared Pathfinder Satellite Observations (CALIPSO) (version 3 level 2); the Cloud Physics Lidar (CPL) optical data products averaged to 1 and 5 km horizontal resolutions. The validation data was collected during the CALIPSO/CloudSat Validation Experiment (CC-VEX) conducted from 26 July to 14 August 2006 from Warner-Robbins, GA.

## Technical Description of Figures:

**Figure 1.** CPL (red) and CALIOP (blue) lidar ratio (extinction to backscatter ratio) frequency distributions during CC-VEX coincident segments (restricted to cases of transparent cirrus with randomly-oriented ice (ROI) conditions only) for the overall distribution (panel a) and the nighttime constrained distribution (panel b). For the overall distribution, most of the cirrus layers analyzed use the default lidar ratio values yielding excellent agreement between the two instruments (value of 25.0 sr). However, when only considering the nighttime constrained retrievals (computed using the transmission loss through the cirrus layer), the retrieved CPL lidar ratio is about 20 sr, or about 5 sr lower than CALIPSO. Also plotted are CPL (red) and CALIOP (green) extinction distributions during CC-VEX coincident segments restricted to transparent ROI conditions only for the overall distribution (panel c) and the distribution where only nighttime constrained lidar ratios are used (panel d). For the overall distribution, excellent agreement between the two instruments is observed as a result of the good agreement in lidar ratio illustrated in (panel a). When considering only the nighttime constrained layers, the retrieved mean CPL extinction is  $0.19 \text{ km}^{-1}$ , which is slightly lower than the CALIPSO retrieved extinction for these layers ( $0.24 \text{ km}^{-1}$ ). This disagreement between extinction for layers using constrained lidar ratios is largely a consequence of the slightly higher disagreement in lidar ratio between the two instruments demonstrated in panel (b). Overall, the optical depth retrievals agree to ~7% but when the constrained retrieval is used at night, the disagreement in optical depth retrievals can be as high as ~31%.

**Scientific significance:** The CALIPSO data products have a large range of applications to significant climate system studies, such as developing global cloud statistics, initializing global cloud models and investigating cloud-aerosol interactions and radiative effects. Therefore, validation of the CALIPSO data products is crucial in quantifying uncertainties and detecting biases in the retrievals and should, in turn, strengthen the results of previous and future studies using CALIPSO data.

**Relevance for future science and relationship to Decadal Survey:** The successful launch of the CALIPSO satellite in April 2006 has provided the science community a five-year global data set of cloud and aerosol properties in the Earth's atmosphere. The primary payload aboard CALIPSO is the Cloud-Aerosol Lidar with Orthogonal Polarization (CALIOP), a dual wavelength elastic backscatter lidar. Reliable optical properties in the standard data products of this lidar instrument is essential for the accurate inclusion in global climate models and future studies of cloud and aerosol climate effects.

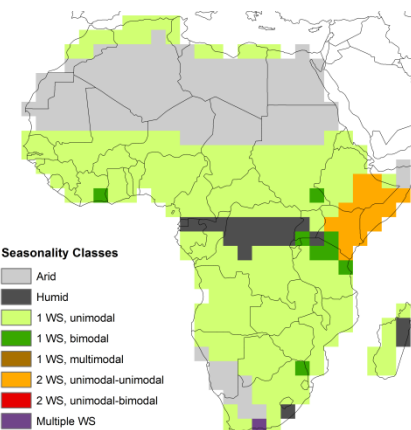
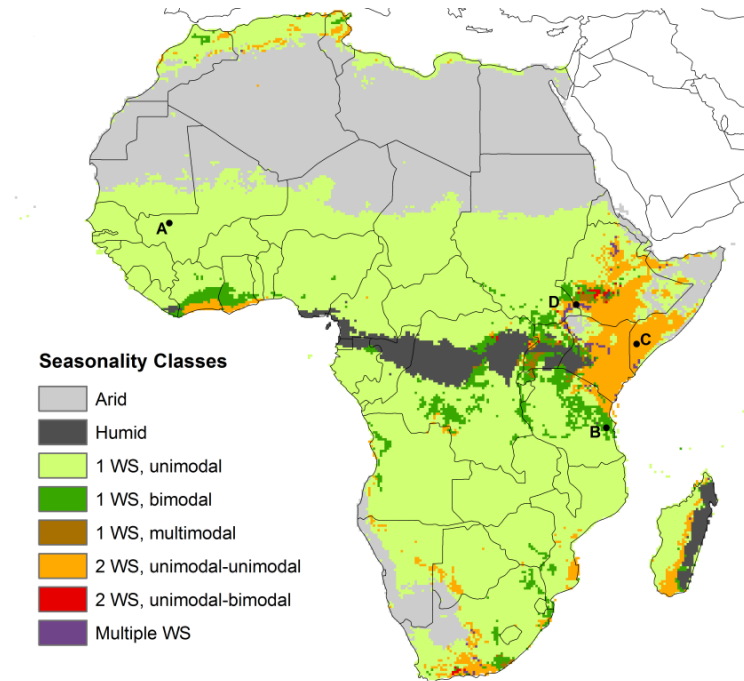


# A New, TRMM-based Analysis of African Rainfall Seasonality

Karen Mohr, Code 612, NASA/GSFC and Stefanie Herrmann, University of Arizona

The wide variety of rainfall regimes in Africa complicates the characterization of trends in both total annual rainfall and its seasonal distribution. The seasonal character of rainfall regimes is of crucial importance to rain-fed agriculture and pasture development in Africa. This study represents the first continental-scale analysis of rainfall seasonality using space-based datasets. From the TRMM Multi-satellite Precipitation Analysis (TMPA), we created a spatially explicit, high-resolution climatology in which the temporal sequence of humid, arid, and dry months determined the seasonality regime.

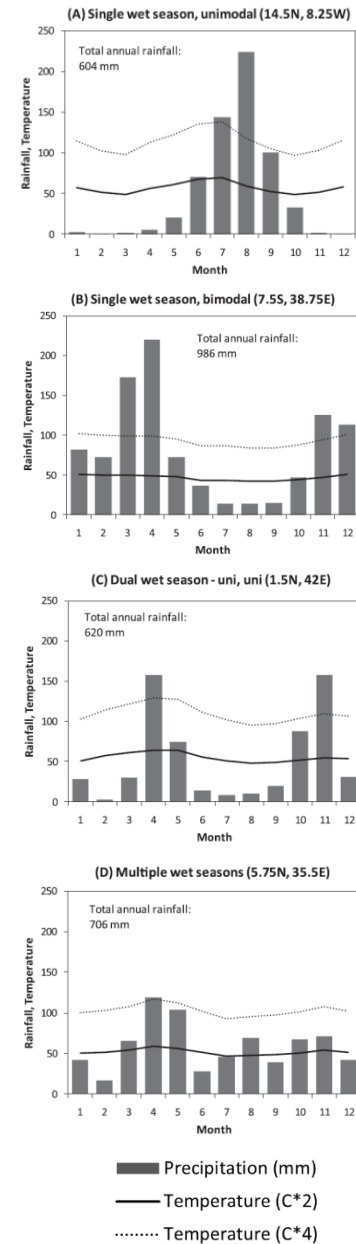
- 8 different seasonality classes were derived from mean monthly rainfall and land surface temperature at 0.25° resolution from the TMPA and MODIS observation periods.
- Seasonal rainfall regimes were more than 60% of the continent, non-seasonal arid regimes were approximately 30%, and non-seasonal wet regimes were less than 5%.
- The TMPA-based analysis was broadly consistent with a longer but coarser resolution GPCP-based analysis and compared well with small regional analyses using station data.

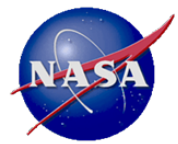


**Figure 3:** Seasonality map based on the GPCP, for comparison to Fig. 1.

**Figure 1:** Seasonality map based on the TMPA, indicating non-seasonal as well as single (1WS), dual (2WS), and multiple wet season regimes and their modalities.

**Figure 2:** Climate diagrams for locations plotted in Fig. 1 A-D. The precipitation and temperature plots determine the seasonality classes of each of these locations. “Humid”  $P \geq 4T_a$ ; “dry”  $2T_a < P < 4T_a$ ; “arid”  $P < 2T_a$ .





Name: Karen Mohr, NASA/GSFC, Code 612  
E-mail: karen.mohr-1@nasa.gov  
Phone: 301-614-6360

### References:

Herrmann, S. M., and K. I. Mohr, 2011: A continental-scale classification of rainfall seasonality regimes in Africa based on gridded precipitation and land surface temperature products. *Journal of Applied Meteorology and Climatology*, **50**, 2504–2513. doi: <http://dx.doi.org/10.1175/JAMC-D-11-024.1>

**Data Sources:** TRMM 3B42 (0.25°, 1997–2010), Global Precipitation Climatology Project (GPCP, 2.5°, 1979–2010), and MODIS monthly mean land surface temperature product (MOD11C3, 0.05°, 2000–2010). Analysis performed in ENVI and IDL.

### Technical Description of Figures:

**Figures 1 and 2:** Fig. 1 is the seasonality map based on the TMPA. Map resolution is 0.25°. The methodology to produce the map and climate diagrams in Fig. 2 was inspired by the canonical bioclimatology of Walter and Lieth (1960), who used empirically derived relationships between precipitation, temperature, and evapotranspiration to define humid and arid months. The definition of dry months was created for this study and represents a condition in which native grasses may experience water stress but not senescence (Todorov et al. 1983; Creswell and Martin 1998). Definitions of dry and wet seasons as well as wet season modality were based on Walter and Lieth (1960) and similar works and then adapted to describe climate diagrams extracted from the TMPA and MOD11C3. Here, a dry season is a consecutive stretch of one or more arid months. A wet season is a consecutive stretch of humid and/or dry months. A single wet season regime is one wet season and one dry season in a year. In a dual wet season regime, two wet seasons alternate with two dry seasons. If more than two wet seasons separated by dry seasons are present, it is a multiple wet season regime. The modality of wet seasons is determined by the presence (or absence) of dry months alternating with humid months. A wet season without dry months is unimodal, and a wet season with one or more dry months between humid months is bimodal.

**Figure 3:** This map is based on the much longer, although coarser resolution, GPCP dataset. The TMPA and GPCP maps are broadly consistent with each other, establishing confidence that the TMPA record is long enough to perform a stable analysis. Other validation included comparing the TMPA map to seasonality studies based on station data, both small-region analyses and the well-cited continental scale analysis by Nicholson et al. (1988).

**Scientific significance:** Evaluating the effects of climate change on rainfall regimes requires a spatially accurate representation of their seasonal climatology to track changes not only in total annual rainfall but also in the seasonal character of rainfall regimes, which is of crucial importance to rain-fed agriculture and pasture development in the semiarid and sub-humid zones. Prior to this study, only selected small (country-scale) and decades-old and very coarse resolution continental analyses using station data were available for Africa. Using gridded, space-based data products, we can characterize rainfall seasonality over Africa at spatial scales relevant to studying seasonality's role as a driver for land cover processes.

**Relevance for future science and relationship to Decadal Survey:** An important aspect of the Precipitation Measuring Mission is the analysis of TRMM and other current satellite-based precipitation information for studies of climate and weather. We demonstrate how the TRMM Multi-satellite Precipitation Analysis (TMPA) can be used to perform continental-scale mapping of seasonal climatology. Such analysis can form the basis for evaluating the implications of climate change on rainfall seasonality regimes and on vegetation phenology within those regimes.





# The first online calculator for atmospheric 3D radiative transfer

T. Várnai, S. Huang, A. Marshak, R. Cahalan, Code 613, NASA GSFC

The Intercomparison of 3D Radiation Codes (I3RC) project sponsored the development of a community model of 3D radiative transfer. This model has now been expanded to create the first online calculator of atmospheric 3D radiative processes. The calculator offers researchers, students, and the public a simple way to perform quick simulations to test new hypotheses and to explore 3D radiative processes. For cloud fields specified by users, the calculator can yield the spatial distribution and scene average value of radiances, fluxes, and absorption at selected visible and near-infrared wavelengths. To help better understand the 3D nature of radiative processes, the calculator can also use an approximation widely used in remote sensing and in dynamical models, and perform 1D calculations for each atmospheric column without considering interactions between columns. Since its public release in January 2012, 100 unique visitors from 15 countries have tried the calculator. The online calculator and the source code of the I3RC community model of 3D radiative transfer are available at <http://i3rc.gsfc.nasa.gov/i3rcmodel>.

Figure 1 shows the simple online interface for setting up calculations. Users can set simulation parameters such as wavelength or solar and view directions using drop-down menus. 3D cloud structure is specified in a text file users need to upload, with the file format following the convention of popular 3D radiation models.

Figure 2 shows a sample result for one of the test cases that were used in the I3RC project for evaluating various simulation techniques. The figure shows the top view of a cumulus cloud field generated through offline dynamical simulations. Colors indicate reflectances at a near-infrared wavelength often used in satellite measurements of cloud particle size and phase. The fact that simulation noise is fairly small reveals that the calculator can provide reliable results through its quick simulations limited to 5 minutes.

**I3RC online calculator**

Wavelength ( $\mu\text{m}$ ): 0.67

Input cloud field(should name "cloud.txt", [sample](#), [readme file](#)) (Choose File) no file selected

Solar zenith angle ( $\theta_0$ )(°) 60

Azimuthal direction of incoming photons ( $\phi_0$ )(°) 0

Viewing zenith angle at which to compute intensity ( $\theta$ )(°) 0

Azimuth of view direction at which to compute intensity ( $\phi$ )(°) 0

Surface albedo 0

Number of photon batches simulated ([read more](#)) 10  
(Each batch includes 100 photons)

Random number seed 1

Radiative calculation ([read more](#)) 1D IPA 3D

Run model Reset

6.4

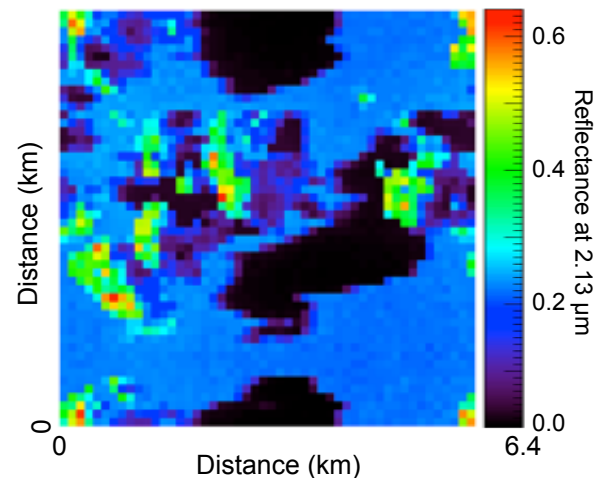
5

Climate and Radiation Bra  
NASA | Goddard | Lab for Atmospher

Hello, [tamas.varnai@nasa.gov](#) Logout

**Figure 1:** User interface for setting up simulations using the online calculator.

**Figure 2:** A sample result from the online calculator. The image shows the calculated reflectance (that is, normalized radiance) field that an observer looking straight down at a cumulus cloud field would see. The sun shines from the left, which results in bright areas in the left side of clouds, and in dark areas both in the right side of clouds and in shadows on the ground.





Name: Tamás Várnai, NASA/GSFC Code 613 and UMBC JCET  
E-mail: [tamas.varnai@nasa.gov](mailto:tamas.varnai@nasa.gov)  
Phone: 301-614-6408

### References:

Cahalan R.F., L. Oreopoulos, A. Marshak, K. F. Evans, A. Davis, R. Pincus, K. Yetzer, B. Mayer, R. Davies, T. Ackerman, H. Barker, E. Clothiaux, R. Ellingson, M. Garay, E. Kassianov, S. Kinne, A. Macke, O'Hirok W., P. Partain, S. Prigarin, A. Rublev, G. Stephens, F. Szczap, E. Takara, T. Várnai, G. Wen, and T. Zhuravleva (2005). The International Intercomparison of 3D Radiation Codes (I3RC): Bringing together the most advanced radiative transfer tools for cloudy atmospheres. *Bull. Amer. Meteor. Soc.*, **86**, 1275-1293.

Pincus, Robert, K. Franklin Evans, 2009: Computational Cost and Accuracy in Calculating Three-Dimensional Radiative Transfer: Results for New Implementations of Monte Carlo and SHDOM. *J. Atmos. Sci.*, **66**, 3131–3146.  
doi: <http://dx.doi.org/10.1175/2009JAS3137.1>

**Figure 1:** User interface for setting up simulations for the online calculator. The illustration at right clarifies the definitions for specifying solar and view directions. Drop-down menus at left set simulation parameters such as wavelength, solar and view directions, surface reflectivity, and simulation length.

**Figure 2:** A sample result from the online calculator. The figure shows the overhead view of reflectances for Case 4, Experiment 4 of I3RC tests that were used for evaluating various simulation techniques. The sun is 30° above the horizon at left, and the surface albedo is 20%. Because cloud droplets are strongly absorbing at the simulated wavelength of 2.13 μm, the shadowy side of clouds appears darker than clear-sky areas. The black areas are shadows on the ground.

**Scientific significance:** Representing the inherently 3D nature of cloud radiative processes is important for improving cloud remote sensing and climate simulations. The new online calculator is the first publicly available online tool for 3D radiative calculations. By enabling quick simulations, it allows researchers to easily test new hypotheses and explore 3D radiative processes, and thus can help improve satellite measurements and climate simulations.

**Educational significance:** By offering an unprecedented simple way for 3D radiative calculations, the online calculator can help a wide range of students learn about the 3D nature of radiative processes and its practical implications.

**Relevance for future science and relationship to Decadal Survey:** Better understanding cloud radiative effects is critical for reducing uncertainties in human impacts on climate, because much of the uncertainties stem from gaps in understanding how anthropogenic aerosols change the radiative impact of clouds. The importance of studying this issue is highlighted in the Decadal Survey, and is a goal for current NASA missions such as Terra or Aqua and future missions such as PACE or ACE.



# New and improved global measurements of fluorescence from space

Joanna Joiner, Yasuko Yoshida, Alexander Vasilkov, Code 614, NASA GSFC,  
Yukio Yoshida, NIES, Japan, Akihiko Kuze, JAXA, Japan,  
Petya Campbell, Lawrence Corp, Elizabeth Middleton, Code 618 NASA GSFC



Since making the first global maps of terrestrial chlorophyll fluorescence in 2011 with the GOSAT Japanese satellite, our group developed a state-of-the-art generalized method to account for complex temporally- and spatially-varying instrumental artifacts to improve the retrievals.

We also examined the filling-in of a broad solar line at 866 nm with moderate spectral resolution SCIAMACHY observations from ESA's EnviSat. The signal is very small, but appears similar to GOSAT-derived fluorescence; it is consistent with fluorescence possibly from chlorophyll though our laboratory measurements were unable to definitively confirm this.

In the afternoon, fluorescence from vegetation is correlated with photosynthesis. [Fluorescence measurements from space may provide estimates of instantaneous photosynthetic activity.](#)

Fluorescence measurements may show plant stress before reductions in greenness take place and are therefore of interest to precision farming, forestry, and carbon assessment.

Fluorescence is a value-added carbon-related product that can be derived from instruments that were not designed to measure it, such as NASA's OCO-2.

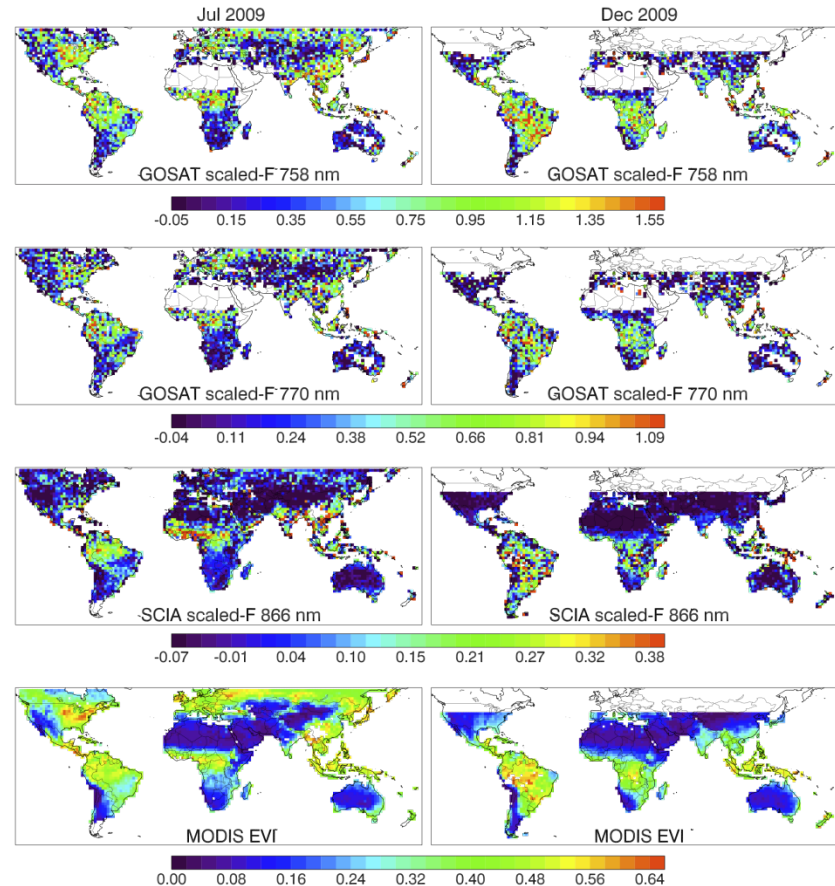


**Figure 1:** Derived fluorescence scaled by incoming photosynthetically-active radiation (PAR) provides an estimate of the relative fluorescence efficiency of vegetation. The expected seasonal shift in photosynthetic activity in 2009 is clearly shown. Right: July 2009; Left: Dec. 2009. Fluorescence is derived from GOSAT in two different spectral windows (top two rows). A similar retrieval performed at a longer wavelengths with SCIAMACHY (3<sup>rd</sup> row). SCIAMACHY shows similar spatial and temporal patterns as compared with GOSAT and the MODIS EVI (a greenness indicator, bottom panels).



Name: Joanna Joiner, NASA/GSFC, Code 614

E-mail: [Joanna.Joiner@nasa.gov](mailto:Joanna.Joiner@nasa.gov)

Phone: 301-614-6247

## References:

Joiner, J., Yoshida, Y., Vasilkov, A. P., and Middleton, E. M., Campbell, P. K. E., Yoshida, Y., Kuze, A., and Corp, L. A., 2012: Filling-in of near-Infrared solar lines by terrestrial fluorescence and other geophysical effects: simulations and space-based observations from SCIAMACHY and GOSAT, in press.

**Data Sources:** Greenhouse-gases Observation “Ibuki” Satellite (GOSAT) Thermal And Near-infrared Sensor for carbon Observation-Fourier Transform Spectrometer (TANSO-FTS), the Scanning Imaging Absorption spectroMeter for Atmospheric CHartographY (SCIAMACHY) satellite instrument onboard the ESA EnviSat and NASA Aqua MODIS enhanced vegetation index

**Technical Description of Figure:** We compare our GOSAT-derived fluorescence information from two different spectral bands on the shoulders of the oxygen A band with the the MODIS Enhanced Vegetation Index (EVI) derived from satellite reflectances. This comparison shows that for several areas these two indices exhibit similar seasonality and/or relative intensity variations, though with some subtle differences. The derived fluorescence therefore provides information that is related to, but independent of the reflectance. We further show an additive signal similarly derived from lower spectral resolution SCIAMACHY measurements at a longer wavelength (866 nm). Fluorescence should be quite low at this wavelength. We were able to measure a fluorescence signal in the laboratory with similar magnitude when the plant was illuminated with a broad-spectrum lamp (solar simulator), but not when stimulated monochromatically by laser (to within instrument sensitivity). [SCIAMACHY signals show similar spatial and temporal variations as compared with GOSAT and MODIS EVI and are therefore consistent with a vegetation source such as chlorophyll fluorescence, though other compounds may fluoresce at this wavelength.](#)

**Scientific significance:** Remote sensing of terrestrial vegetation fluorescence from space is of interest because it can potentially provide global coverage of the functional status of vegetation. For example, fluorescence observations may provide a means to detect vegetation stress before chlorophyll reductions take place. Although there have been many measurements of fluorescence from ground- and airborne-based instruments, there has been scant information available from satellites until our initial work with GOSAT. Since then, several other groups have been working with GOSAT data and various methods have been employed to correct for instrumental artifacts. In this work, we use high-spectral resolution data GOSAT that is in a sun-synchronous orbit with an equator crossing time near 13:00 LT. We use filling-in of the strong potassium (K) I solar Fraunhofer line near 770 nm and other solar lines near 758 nm to derive chlorophyll fluorescence and related parameters at those wavelengths. We also examine the filling-in of the Ca II line at 866 nm with SCIAMACHY. This is the only wide and deep line in the NIR not contaminated by water vapor. [We develop and employ a general state-of-the-art method to both GOSAT and SCIAMACHY data that is able to account for complex temporally- and spatially-varying instrumental artifacts.](#)

This work is an important step forward in demonstrating that the health of terrestrial ecosystems can be monitored from space. Our research provides a basis for future satellite missions specifically designed to measure vegetation fluorescence such as the Florescence Explorer (FLEX) mission that was selected for assessment by the European Space Agency (ESA) in 2006. [Finally, our work shows that potentially lower cost instrumentation \(moderate spectral resolution\) can be potentially used to derive fluorescence information from aircraft and ground \(and potentially from space\) with a relatively simple algorithm \(i.e., complex atmospheric correction is not necessary\).](#)

**Relevance for future science and relationship to Decadal Survey:** It will also be possible to retrieve fluorescence at a higher spatial resolution and with less cloud contamination using the NASA Orbiting Carbon Observatory-2 (OCO-2) to be launched in the next few years. Fluorescence will be an important value-added carbon-related product from OCO-2. There is currently no decadal survey mission specifically designed to measure fluorescence.